Journal of Crystal Growth 51 (1981) 557–567
© North-Holland Publishing Company

RATE CHANGE TRANSIENTS IN BRIDGMAN–STOCKBARGER GROWTH

Ta-Wei FU and William R. WILCOX
Department of Chemical Engineering, Clarkson College of Technology, Potsdam, New York 13676, USA

Received 30 June 1980; manuscript received in final form 23 September 1980

Thermal steady state in a Bridgman–Stockbarger crystal growth system is perturbed by a sudden increase of the ampoule moving rate. An explicit finite difference numerical scheme was developed for the one-dimensional transient state heat transfer computation of such a perturbation. The temperature field inside the ampoule, and the solid/liquid interface position, were computed versus time from the rate change. It was found that the transient behavior of the freezing rate strongly depended on the Biot numbers of the system, dimensionless latent heat, and the thickness of the insulation in between the heater and the cooler. The numerical results were well correlated by an equation, which can be used to estimate the time required for the freezing rate to equal the new moving rate.

1. Introduction

It has long been known that the microstructure of a directionally solidified eutectic depends on the solidification rate and perhaps also the temperature gradient at the solid/liquid interface [1,2]. A Bridgman–Stockbarger apparatus may be used to perform the directional solidification under controlled conditions. A tube or ampoule containing melt and solid is slowly lowered from a heater into a cooler, as shown in fig. 1. At steady state, the solidification rate equals the ampoule moving rate, i.e., the solid/liquid interface position is stationary relative to the heater and cooler.

Recently, some researchers have become interested in applying sudden rate changes of the ampoule in order to force the crystal to grow at several different rates along one ampoule [3]. The variation of the microstructure of eutectic alloys caused by a continuous change of solidification rate has also been investigated [4]. A sudden change of the ampoule moving rate perturbs the thermal steady state inside the ampoule. Without end effects, the thermal field inside the ampoule is expected to go through a transition period toward a second thermal steady state. The solid/liquid interface is also expected to shift from the first steady state position to a second steady state position. The crystal growth rate differs from the ampoule moving rate during this thermal transition period.

In the present study, the transient behavior of the solid/liquid interface movement after a sudden increase of the ampoule moving rate was studied for a simplified furnace model. Our attention was devoted primarily to growth of metallic systems, which usu-

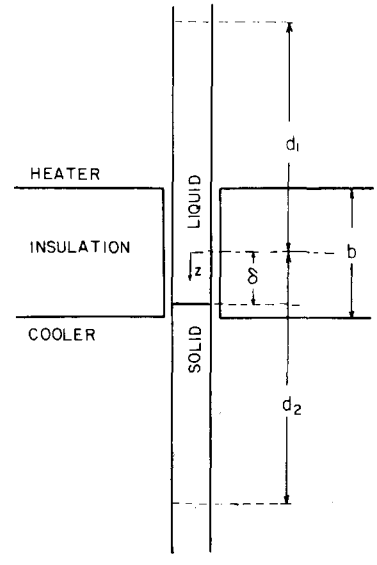

Fig. 1. Coordinate system.

ally have low Biot numbers ranging from 0.01 to 0.1. With a small Biot number, the heat transfer is predominantly axial, permitting us to use a one-dimensional model in which temperature varies with axial position only and not radially.

2. Analysis

The coordinate system is shown in fig. 1. The one-dimensional unsteady state differential equation for temperature T is

$$k\frac{\partial^2 T}{\partial z^2} - VC_p\rho\frac{\partial T}{\partial z} - \frac{2h}{a}(T - T_a) = C_p\rho\frac{\partial T}{\partial t}, \qquad (1)$$

where k is the thermal conductivity, ρ is the density, V is the ampoule moving rate, C_p is the heat capacity, h is the heat transfer coefficient through the ampoule wall, a is the radius, T_a is the temperature of the environment (heater or cooler), t is the time coordinate, and z is the axial space coordinate. The origin of the z coordinate is fixed at the center of the insulation. The dimensionless form of this equation is

$$K^L\frac{\partial^2\phi}{\partial Z^2} - \mathrm{Pe}^L\frac{\partial\phi}{\partial Z} - 2H^L(\phi - \phi^a) = \frac{\partial\phi}{\partial\theta}, \qquad (2)$$

where

$\phi = (T - T_c)/(T_h - T_c)$

(dimensionless temperature),

$\phi^a = (T_a - T_c)/(T_h - T_c)$

(dimensionless temperature of environment),

$Z = z/a$ (dimensionless space coordinate),

$K^L = k/k^L$

(dimensionless thermal conductivity),

$\mathrm{Pe}^L = VC_p\rho a/k^L$ (Péclet number),

$H^L = ha/k^L$ (Biot number),

$\theta = (k^L/C_p\rho a^2)\,t$ (dimensionless time),

k^L = thermal conductivity of the melt at the melting temperature.

The energy balance equation at the solid/liquid interface is

$$k^L\left.\frac{\partial T}{\partial z}\right|_L + V\rho\,\Delta H - \frac{d\delta}{dt}\rho\,\Delta H = k^S\left.\frac{\partial T}{\partial z}\right|_S, \qquad (3)$$

where $\partial T/\partial z|_L$ and $\partial T/\partial z|_S$ are the temperature gradients at the interface in the melt and in the solid, respectively, ΔH is the latent heat of solidification, δ is the interface position relative to the centerline of the insulation, and k^S is the thermal conductivity of the solid at the melting temperature. The energy balance equation at the solid/liquid interface can be written in dimensionless form as

$$\frac{d\bar{\delta}}{d\theta} = \frac{1}{W_b}\left[K\left.\frac{d\phi}{d\eta}\right|_S - \left.\frac{d\phi}{d\eta}\right|_L\right] + \mathrm{Pe}^L, \qquad (4)$$

where

$\bar{\delta} = \delta/a$ (dimensionless interface position),

$W_b = \Delta H/C_p(T_h - T_c)$

(dimensionless latent heat),

$K = k^S/k^L$.

An explicit finite difference computational scheme was developed to compute the temperature profile, as well as the solid/liquid interface position, versus time after a sudden increase of the ampoule moving rate. The details of the finite difference formulation are given in the appendix.

The assumptions of the present study are:

(i) The density and the heat capacity are the same in the liquid and in the solid, and independent of temperature.

(ii) The thermal conductivity is constant in the liquid and in the solid, although not necessarily equal to one another.

(iii) Interface supercooling is neglected.

(iv) The heat transfer coefficient h at the ampoule wall is constant in the heater and in the cooler, although not necessarily the same in both.

(v) The ampoule is sufficiently long that end effects may be neglected (~6 tube diameters both above and below the insulated region).

The temperature profile at steady state ($\partial T/\partial t = 0$) can be calculated analytically [5,6]. Thus, the initial values at all grid points in the finite difference scheme were calculated from this analytical solution. Since the temperature along the ampoule approaches the temperature of the heater asymptotically with

decreasing Z, and approaches the cooler temperature asymptotically with increasing Z, the proper values of d_1 and d_2 can be chosen such that the space coordinate used in the finite difference computational scheme varies from $Z = -d_1/a$ to $Z = d_2/a$. The values of d_1 and d_2 were chosen in such a way that

(a) $\phi > 0.9995$ at $Z = -d_1/a$,

(b) $\phi < 0.0005$ at $Z = d_2/a$,

for the initial steady state. (These values of d_1 and d_2 were large enough so that it was not necessary to increase d_1 or d_2 during the computation.) The use of larger values of d_1 and d_2 provided only very slightly greater accuracy at the expense of a significant increase in computing time.

3. Results without insulation between heater and cooler

The thickness of the insulation in between the heater and the cooler is assumed to be negligible in all the cases reported in this section. Fig. 2 is a typical plot of the relation between the dimensionless interface position and the dimensionless time after a sudden increase of the ampoule moving rate, for different values of the dimensionless interface temperature ϕ_m. It appears that the solid/liquid interface moves from the first steady state position $\bar{\delta}_1$ toward the second steady state position $\bar{\delta}_2$ asymptotically.

An interfacial position parameter is defined as $P = (\bar{\delta}_2 - \bar{\delta})/(\bar{\delta}_2 - \bar{\delta}_1)$ in order to characterize the results. Semi-logarithmic plots of the dependence of P versus dimensionless time θ appear to be very close to a straight line connecting the data points at $\theta = 0$ and $\theta = 10$ for all the investigated cases, as shown in fig. 3 to fig. 7. Thus, the relation between the interface position parameter and the dimensionless time can be expressed by an exponential relation,

$$P = (\bar{\delta}_2 - \bar{\delta})/(\bar{\delta}_2 - \bar{\delta}_1) = \exp(-2.303A\theta) , \qquad (5)$$

where A is the absolute value of the slope of the straight lines. From eqs. (2) and (4), we can write the functional dependence as

$$A = f(H^{hL}, H^{cL}, W_b, \phi_m, Pe^{L1}, Pe^{L2}, K) , \qquad (6)$$

where $H^{hL}(= h_h a/k^L)$ is the Biot number in the heater, $H^{cL}(= h_c a/k^L)$ is the Biot number in the cooler, $Pe^{L1}(= V_1 C_p \rho a/k^L)$ is the Péclet number before the sudden change of the ampoule moving rate, and $Pe^{L2}(= V_2 C_p \rho a/k^L)$ is the Péclet number after the sudden change of the ampoule moving rate.

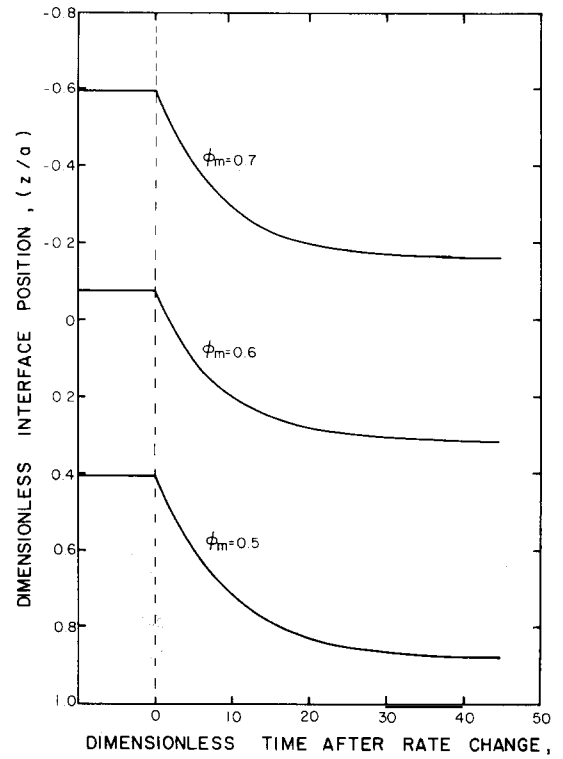

Fig. 2. Dimensionless interface position versus dimensionless time after the change of the ampoule moving rate ($H^{hL} = H^{cL} = 0.1, K = 1.0, W_b = 1.0, Pe^{L1} = 0.05, Pe^{L2} = 0.1$).

Figs. 3 to 7 are plots for $H^{hL} = H^{cL}$. Figs. 3 and 4 show the influence on slope A of the Biot number (dimensionless heat transfer coefficient at the ampoule wall) and the latent heat of solidification. The value of A increases with increasing dimensionless heat transfer coefficient and decreases with increasing dimensionless latent heat.

Fig. 5 shows the behavior of the interfacial position parameter P for different values of the dimensionless interface temperature ϕ_m, The straight line was drawn for $\phi_m = 0.6$. Even though the data points for $\phi_m = 0.5$ deviate from a straight line to some extent, a negligible dependence of the interfacial movement on the dimensionless interface tempera-

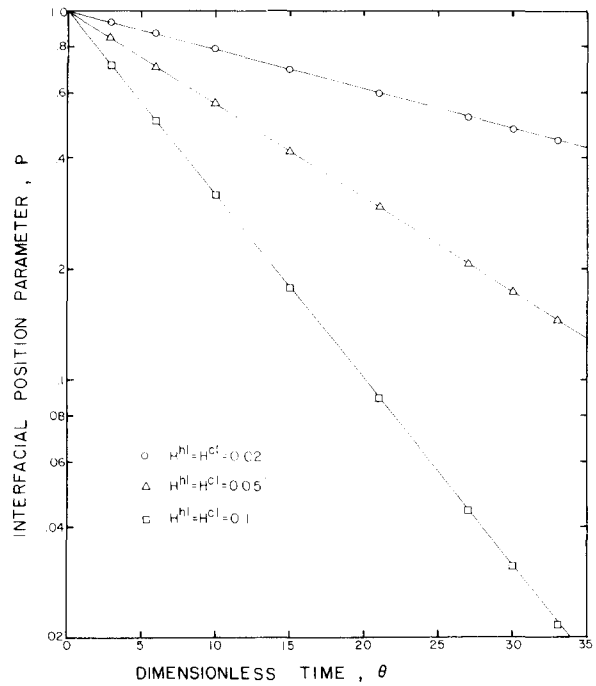

Fig. 3. Interfacial position parameters versus dimensionless time for different Biot numbers ($\phi_m = 0.6$, $K = 1.0$, $W_b = 1.0$, $Pe^{L1} = 0.01$, $Pe^{L2} = 0.02$).

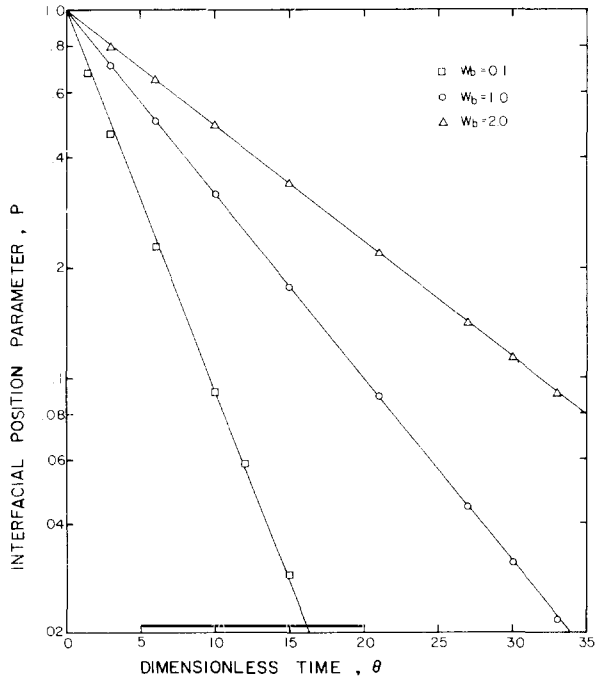

Fig. 4. Interfacial position parameter versus dimensionless time for different values of dimensionless latent heat ($H^{hL} = H^{cL} = 0.1$, $\phi_m = 0.6$, $K = 1.0$, $Pe^{L1} = 0.01$, $Pe^{L2} = 0.02$).

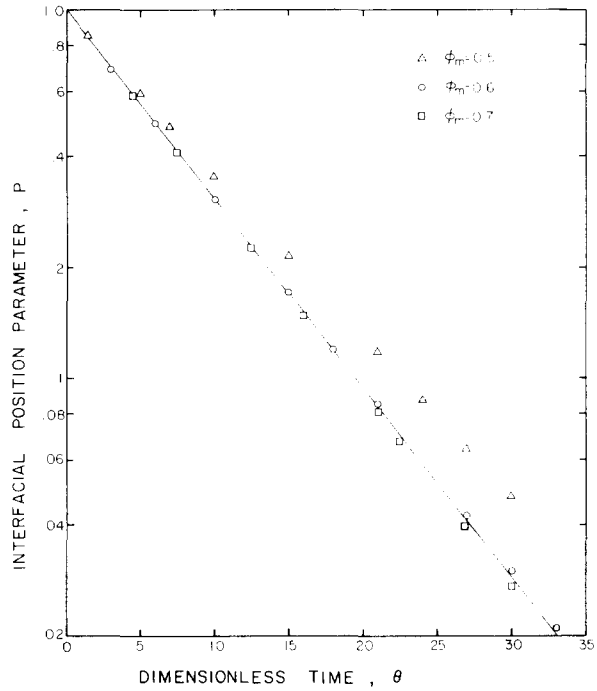

Fig. 5. Interfacial position parameters versus dimensionless time for different values of the dimensionless interface temperature ($H^{hL} = H^{cL} = 0.1$, $K = 1.0$, $W_b = 1.0$, $Pe^{L1} = 0.05$, $Pe^{L2} = 0.1$).

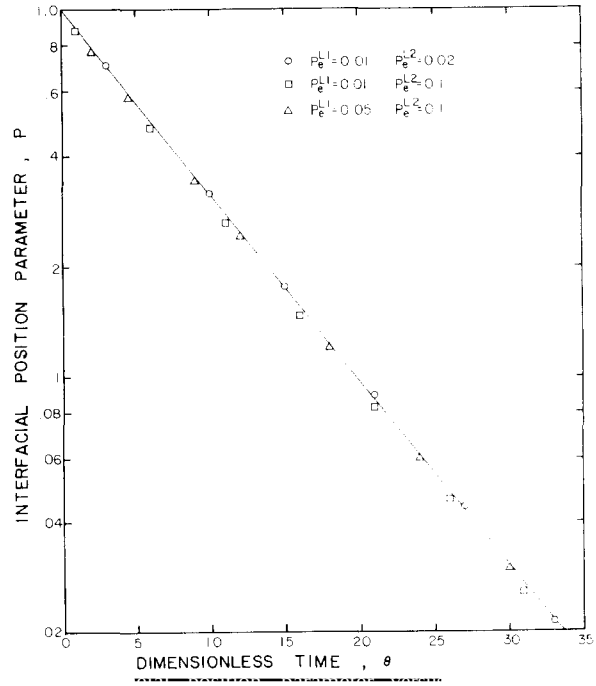

Fig. 6. Interfacial position parameter versus dimensionless time for different combinations of dimensionless ampoule moving rates before and after the sudden change of the ampoule moving rate ($H^{hL} = H^{cL} = 0.1$, $\phi_m = 0.6$, $K = 1.0$, $W_b = 1.0$).

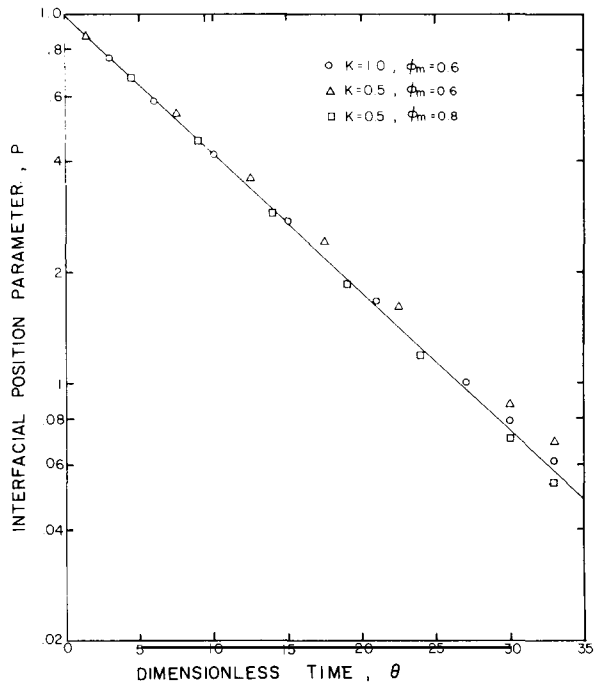

Fig. 7. Interfacial position parameters versus dimensionless time for different ratios of the thermal conductivity in solid to that in liquid ($H^{hL} = H^{cL} = 0.05$, $W_b = 0.5$, $Pe^{L1} = 0.05$, $Pe^{L2} = 0.1$).

ture ϕ_m can still be seen. Actually, we found that the behavior of P is almost unaffected by ϕ_m when the interface is near the heater–cooler boundary. Fortunately, we normally desire a planar interface shape, which occurs when the interface is near the heater–cooler boundary.

Different combinations of the dimensionless ampoule moving rates before and after the sudden change do not affect the behavior of P, as shown in fig. 6. Similarly, different thermal conductivities of the liquid and the solid do not significantly influence the behavior of P, as shown in fig. 7. The minor deviation of the data points for different cases in figs. 6 and 7 is attributed to the variation of the interface position from case to case.

Since ϕ_m, Pe^{L1}, Pe^{L2} and K have only a slight influence on P versus θ, eq. (6) can be simplified to

$$A = f(H^{hL}, H^{cL}, W_b) . \tag{7}$$

Fig. 8 shows the values of A for the 18 cases studied. It appears that A depends linearly on Biot number H^L for the same value of dimensionless latent heat W_b. The straight lines in fig. 8 are least square fits of data points with the same value of W_b. The slope of these straight lines increase with decreasing W_b. A correlating equation which expresses the dependence of A on the dimensionless latent heat W_b and the Biot number H^L is

$$A = H^L \exp(0.4325 - 1.1187 W_b^{1/2}) , \tag{8}$$

where

$$H^L = H^{hL} = H^{cL} .$$

For $H^{hL} \neq H^{cL}$, good results were obtained by substituting the geometric mean of H^{hL} and H^{cL} for H^L in eq. (8). Thus, eq. (8) can be written as

$$A = H^{Lm} \exp(0.4325 - 1.1187 W_b^{1/2}) , \tag{9}$$

where $H^{Lm} = (H^{hL} H^{cL})^{1/2}$. Fig. 9 shows comparison of the numerical results for P versus θ with those predicted by the correlating relations, eqs. (5) and (9), for $H^{hL} \neq H^{cL}$.

It can further be shown that

$$\frac{V_2 - V_S}{V_2 - V_1} = \frac{\bar{\delta}_2 - \bar{\delta}}{\bar{\delta}_2 - \bar{\delta}_1} = P = \exp(-2.303 A\theta) \tag{10}$$

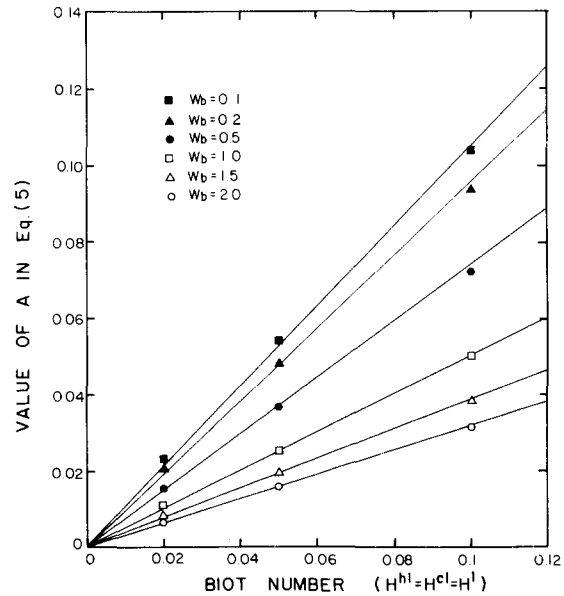

Fig. 8. Slope of the straight line on the semi-logarithmic plot, P versus θ, versus dimensionless heat transfer coefficient for different values of dimensionless latent heat ($\phi_m = 0.6$, $K = 1.0$, $Pe^{L1} = 0.01$, $Pe^{L2} = 0.02$).

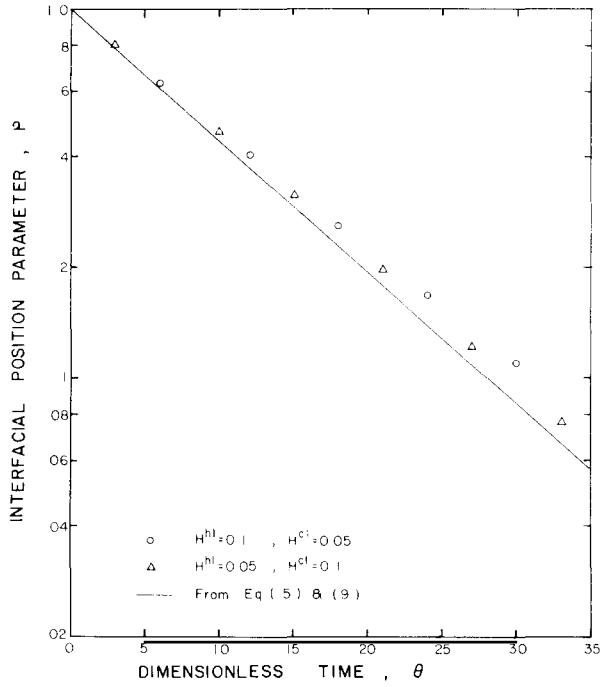

Fig. 9. Comparison between the interfacial position parameter calculated from eqs. (5) and (9) and that computed from the numerical scheme for the cases that $H^{hL} \neq H^{cL}$ (ϕ_m = 0.6, K = 1.0, W_b = 1.0, Pe^{L1} = 0.01, Pe^{L2} = 0.05).

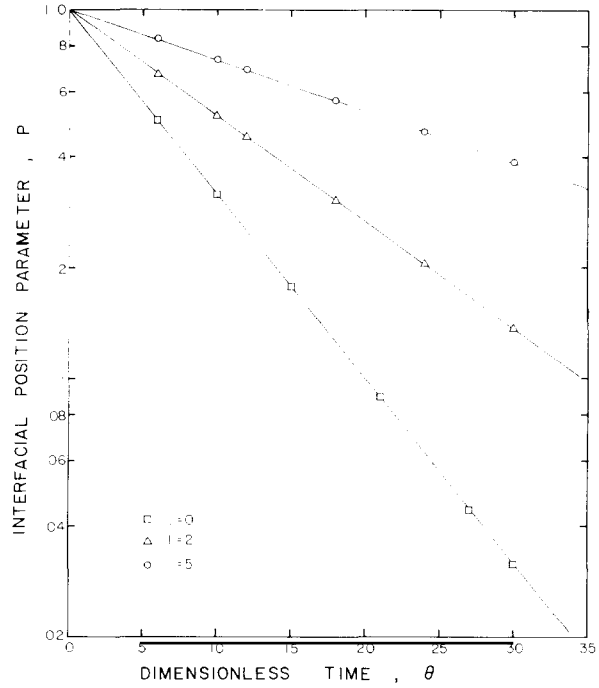

Fig. 10. Interfacial position parameter versus dimensionless time for different thickness of the insulation ($H^{hL} = H^{cL}$ = 0.1, ϕ_m = 0.6, K = 1.0, W_b = 1.0, Pe^{L1} = 0.01, Pe^{L} = 0.02).

where V_1 and V_2 are ampoule moving rates before and after the sudden change, respectively, and V_S is the solidification rate. The time required for the solidification rate to reach a certain value can also be calculated from eq. (10).

4. Effect of insulation

The behavior of the interfacial position parameter P strongly depends on the thickness of the insulation between the heater and the cooler, as shown in fig. 10. It was also found that Pe^{L1}, Pe^{L2}, K, and ϕ_m did not have a significant effect on the behavior of P so long as the interface remains in the neigborhood of the insulated region. An extension of eq. (5) gives an expression for the functional dependence of the interfacial position parameter:

$$\frac{\log[(\bar{\delta}_2 - \bar{\delta})/(\bar{\delta}_2 - \bar{\delta}_1)]}{-A\theta} = g(I, H^{Lm}, W_b) , \qquad (11)$$

where I is the dimensionless thickness of the insulation. Note that

$$\log[(\bar{\delta}_2 - \bar{\delta})/(\bar{\delta}_2 - \bar{\delta}_1)]/\theta$$

is the slope of the straight line connecting the data points at θ = 0 and θ = 10 on a semi-logarithmic plot of P versus θ. A linear regression procedure [7] was performed for the 27 tested cases listed in table 1 to derive a correlating equation for the function $g(I, H^{Lm}, W_b)$. It was found to be well correlated by

$$g = \exp[-I(0.0774 + 1.6858H^{Lm} + 0.0184W_b)] , \qquad (12)$$

with a correlation coefficient r of 0.998. Thus, the interfacial position parameter can be expressed as

$$P = (\bar{\delta}_2 - \bar{\delta})/(\bar{\delta}_2 - \bar{\delta}_1) = \exp[-2.303B\theta] , \qquad (13)$$

where

$$B = H^{Lm} \exp(0.4325 - 1.1187W_b^{1/2} - 0.0774I - 1.6858IH^{Lm} - 0.0184IW_b) .$$

Table 1
Computer results used to derive the correlating equation for the function $g(I, H^{Lm}, W_b)$; $\phi_m = 0.6$, $Pe^{L1} = 0.01$, and $Pe^{L2} = 0.02$

H^{hL}	H^{cL}	W_b	I	$\log P/(-A\theta)$
0.1	0.1	1.0	2.0	0.572
0.1	0.1	0.5	3.0	0.477
0.1	0.1	1.0	3.0	0.433
0.1	0.1	2.0	3.0	0.403
0.1	0.1	1.0	4.0	0.340
0.1	0.1	0.5	5.0	0.301
0.1	0.1	1.0	5.0	0.270
0.1	0.1	2.0	5.0	0.254
0.1	0.1	1.0	6.0	0.221
0.05	0.05	1.0	2.0	0.675
0.05	0.05	0.5	3.0	0.596
0.05	0.05	1.0	3.0	0.545
0.05	0.05	2.0	3.0	0.517
0.05	0.05	1.0	4.0	0.447
0.05	0.05	0.5	5.0	0.411
0.05	0.05	1.0	5.0	0.373
0.05	0.05	2.0	5.0	0.357
0.05	0.05	1.0	6.0	0.315
0.02	0.02	1.0	2.0	0.801
0.02	0.02	0.5	3.0	0.745
0.02	0.02	1.0	3.0	0.689
0.02	0.02	2.0	3.0	0.680
0.02	0.02	1.0	4.0	0.599
0.02	0.02	0.5	5.0	0.569
0.02	0.02	1.0	5.0	0.524
0.02	0.02	2.0	5.0	0.527
0.02	0.02	1.0	6.0	0.463

Furthermore, the relation between the solidification rate and the dimensionless time can also be expressed as

$$(V_2 - V_S)/(V_2 - V_1) = \exp(-2.303B\theta) \qquad (14)$$

5. Discussion and conclusion

The interfacial position parameter $P = (\bar{\delta}_2 - \bar{\delta})/(\bar{\delta}_2 - \bar{\delta}_1)$ was used to describe the transient behavior of the interface movement after a sudden increase of the sample moving rate in the Bridgman–Stockbarger crystal growth system. It was found that the transient behavior strongly depends on the Biot number in the heater and in the cooler, dimensionless latent heat, and the thickness of the insulation between the heater and the cooler. A correlating equation was derived to describe the relation between P and dimensionless time θ. The time required for the solidification rate to reach a certain value after the sudden increase of the ampoule moving rate can also be estimated from

$$\theta = -B^{-1} \log[(V_2 - V_S)/(V_2 - V_1)] . \qquad (15)$$

Thus, the time required to reach a new steady state is decreased by having a large temperature difference between the heater and the cooler, effective heat transfer between ampoule and furnace, and no insulated region between the heater and the cooler. Unfortunately, we have shown previously [8] that an insulated zone is very useful in producing an interface shape that is nearly planar, and that it reduces the sensitivity of interface shape to changes in operating conditions. The time required for the freezing rate to "catch up" with a new ampoule movement rate does not depend on either the initial movement or the final movement rate.

We suspect that the response to a change in heater or cooler temperature will have the same time constant as for the mechanical effect described here. However, computations are needed to check on this.

Appendix

An explicit finite difference scheme was used. In space coordinates, the three-points central difference forms were employed for the first and the second derivatives, i.e.

$$\frac{\partial^2 \phi}{\partial Z^2} = \frac{\phi_{i+1,j} - 2\phi_{i,j} + \phi_{i-1,j}}{(\Delta Z)^2} , \qquad (A.1)$$

$$\frac{\partial \phi}{\partial Z} = \frac{\phi_{i+1,j} - \phi_{i-1,j}}{2\,\Delta Z} . \qquad (A.2)$$

The first derivative of time was expressed as

$$\frac{\partial \phi}{\partial \theta} = \frac{\phi_{i,j+1} - \phi_{i,j}}{\Delta \theta} , \qquad (A.3)$$

$$\frac{\partial \bar{\delta}}{\partial \theta} = \frac{\Delta \bar{\delta}}{\Delta \theta} . \qquad (A.4)$$

where $\Delta\bar{\delta}$ is the movement of the interface in the time step $\Delta\theta$. Substituting eq. (A.4) into eq. (4), the

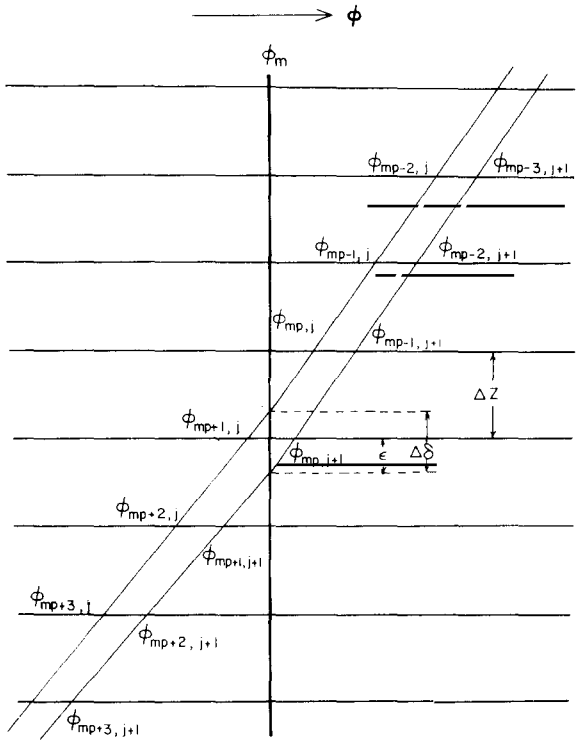

Fig. 11. Grid system at the neighborhood of the solid/liquid interface. (Interface does not cross any grid point in a time step.)

interface movement $\Delta\bar{\delta}$ in each time step $\Delta\theta$ can be expressed as

$$\Delta\bar{\delta} = \left[\frac{1}{W_b}\left(K\frac{d\phi}{dZ}\bigg|_S - \frac{d\phi}{dZ}\bigg|_L\right) + Pe^L\right]\Delta\theta \,. \qquad (A.5)$$

The temperature at the neighboring grid points of the solid/liquid interface was computed for the following different cases:

(i) The interface does not cross any grid point in the time step $\Delta\theta$ (as shown in fig. 11): Lagrange's interpolation is used to compute the temperature at grid point mp

$$\phi_{mp,j+1} = \frac{-Y}{2+Y}\phi_{mp-2,j+2} + \frac{2Y}{1+Y}\phi_{mp-1,j+1} + \frac{2}{(2+Y)(1+Y)}\phi_m \qquad \text{for } Y \leqslant \tfrac{1}{2} \,,$$

and the temperature at grid point mp + 1

$$\phi_{mp+1,j+1} = \frac{2(1-Y)}{2-Y}\phi_{mp+2,j+1} + \frac{-1+Y}{3-Y}\phi_{mp+3,j+1} + \frac{2}{(2-Y)(3-Y)}\phi_m \qquad \text{for } Y > \tfrac{1}{2} \,,$$

where

$$\phi_m = (T_m - T_c)/(T_h - T_c) \,, \qquad Y = \epsilon/\Delta z \,.$$

When $Y > \frac{1}{2}$, $\phi_{mp,j+1}$ is computed from the finite difference form of eq. (2) as

$$\phi_{mp,j+1} = \left[K^L\frac{\Delta\theta}{(\Delta Z)^2} - \frac{1}{2}Pe^L\frac{\Delta\theta}{\Delta Z}\right]\phi_L + \left[K^L\frac{\Delta\theta}{(\Delta Z)^2} + \frac{1}{2}Pe^L\frac{\Delta\theta}{\Delta Z}\right]\phi_{mp-1,j} + \left[1 - 2K^L\frac{\Delta\theta}{(\Delta Z)^2} - 2H^L\Delta\theta\right]\phi_{mp,j} + 2H^L_{mp,j}\Delta\theta\phi^a_{mp,j} \,,$$

where ϕ_L is the extrapolated temperature at grid point mp + 1 from the temperature at grid points mp, mp − 1, mp − 2 and the interface

$$\phi_L = \frac{6}{Y(1+Y)(2+Y)}\phi_m + \frac{3(1-Y)}{-Y}\phi_{mp,j} + \frac{3(1-Y)}{1+Y}\phi_{mp-1,j} + \frac{1-Y}{2-Y}\phi_{mp-2,j} \,.$$

When $Y \leqslant \frac{1}{2}$, $\phi_{mp+1,j+1}$ is computed from the finite difference form of eq. (2) as

$$\phi_{mp+1,j+1} = \left[K^L\frac{\Delta\theta}{(\Delta Z)^2} - \frac{1}{2}Pe^L\frac{\Delta\theta}{\Delta Z}\right]\phi_{mp+2,j} + \left[K^L\frac{\Delta\theta}{(\Delta Z)^2} + \frac{1}{2}Pe\frac{\Delta\theta}{\Delta Z}\right]\phi_S + \left[1 - 2K^L\frac{\Delta\theta}{(\Delta Z)^2} - 2H^L_{mp+1,j}\Delta\theta\right]\phi_{mp+1,j} + 2H^L_{mp+1,j}\Delta\theta\,\phi^a_{mp+1} \,,$$

where ϕ_S is the extrapolated temperature at grid point mp from the temperature at grid points mp + 1, mp + 2, mp + 3 and the interface

$$\phi_S = \frac{6}{(1-Y)(2-Y)(3-Y)}\phi_m + \frac{-3Y}{1-Y}\phi_{mp+1,j}$$

$$+\frac{3Y}{2-Y}\phi_{mp+2,j}+\frac{-Y}{3-Y}\phi_{mp+3,j}\,.$$

(ii) The interface crosses a grid point in a time step $\Delta\theta$ (as shown in fig. 12):

$$\phi_{mp-1,j+1}=\left[K^{L}\frac{\Delta\theta}{(\Delta Z)^2}-\frac{1}{2}\mathrm{Pe}^{L}\frac{\Delta\theta}{\Delta Z}\right]\phi_{L}$$
$$+\left[K^{L}\frac{\Delta\theta}{(\Delta Z)^2}+\frac{1}{2}\mathrm{Pe}^{L}\frac{\Delta\theta}{\Delta Z}\right]\phi_{mp-2,j}$$
$$+\left[1-2K^{L}\frac{\Delta\theta}{(\Delta Z)^2}-2H^{L}_{mp-1,j}\,\Delta\theta\right]\phi_{mp-1,j}$$
$$+2H^{L}_{mp-1,j}\,\Delta\theta\,\phi^{a}_{mp,j}\,,$$

$$\phi_{mp,j+1}=\frac{Y}{2+Y}\phi_{mp-2,j+1}+\frac{2Y}{1+Y}\phi_{mp-1,j+1}$$
$$+\frac{2}{(2+Y)(1+Y)}\phi_{m}\,.$$

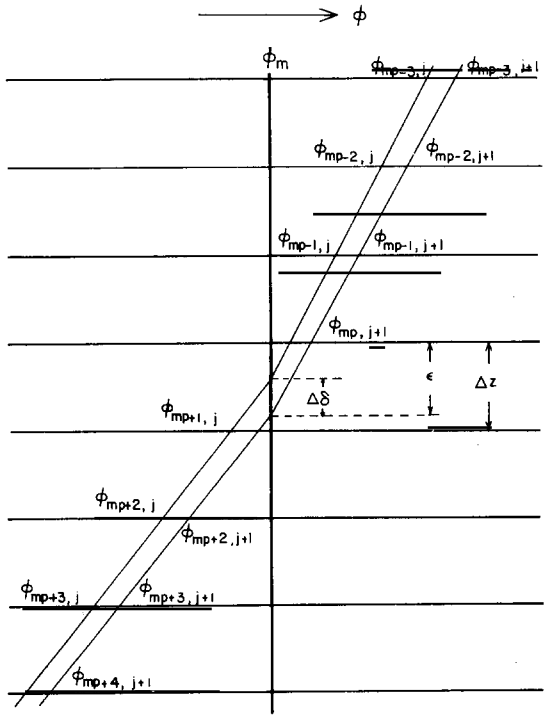

Fig. 12. Grid system at the neighborhood of the solid/liquid interface. (Interface crosses a grid point in a time step.)

The temperature gradients at the solid/liquid interface, $\mathrm{d}\phi/\mathrm{d}Z|_{S}$ and $\mathrm{d}\phi/\mathrm{d}Z|_{L}$, have to be calculated in order to use eq. (A.5) to calculate the interface movement in each time step. The temperature in the liquid side is

$$\left.\frac{\mathrm{d}\phi}{\mathrm{d}Z}\right|_{L}=Y\left(\frac{\mathrm{d}\phi}{\mathrm{d}Z}\right)_{L1}+(1-Y)\left(\frac{\mathrm{d}\phi}{\mathrm{d}Z}\right)_{L2}\,,$$

where $(\mathrm{d}\phi/\mathrm{d}Z)_{L1}$ is computed from the temperature at grid points mp, mp − 1, mp − 2, and the interface $(\mathrm{d}\phi/\mathrm{d}Z)_{L2}$ is computed from the temperature at grid points mp − 1, mp − 2, mp − 3 and the interface (as shown in fig. 11). Lagrange's interpolation function can be formed from the temperature at grid points mp, mp − 1, mp − 2 and the interface (or grid points mp − 1, mp − 2, mp − 3 and the interface). The temperature gradients at the interface, $(\mathrm{d}\phi/\mathrm{d}Z)_{L1}$ and $(\mathrm{d}\phi/\mathrm{d}Z)_{L2}$, can be computed from the first derivative of the aforementioned Lagrange's interpolation function

$$\left(\frac{\mathrm{d}\phi}{\mathrm{d}Z}\right)_{L1}=\left(\frac{1}{2+Y}+\frac{1}{1+Y}+\frac{1}{Y}\right)\frac{1}{\Delta Z}\phi_{m}$$
$$-\frac{(1+Y)(2+Y)}{2Y}\frac{1}{\Delta Z}\phi_{mp}$$
$$+\frac{Y(2+Y)}{1+Y}\frac{1}{\Delta Z}\phi_{mp-1}-\frac{Y(1+Y)}{2(2+Y)}\frac{1}{\Delta Z}\phi_{mp-2}\,,$$

$$\left(\frac{\mathrm{d}\phi}{\mathrm{d}Z}\right)_{L2}=\left(\frac{1}{1+Y}+\frac{1}{2+Y}+\frac{1}{3+Y}\right)\frac{1}{\Delta Z}\phi_{m}$$
$$-\frac{(2+Y)(3+Y)}{2(1+Y)}\frac{1}{\Delta Z}\phi_{mp-1}$$
$$-\frac{(1+Y)(3+Y)}{2+Y}\frac{1}{\Delta Z}\phi_{mp-2}$$
$$-\frac{(1+Y)(2+Y)}{2(3+Y)}\frac{1}{\Delta Z}\phi_{mp-3}\,.$$

Similarly, the temperature gradient on the solid side is

$$\left.\frac{\mathrm{d}\phi}{\mathrm{d}Z}\right|_{S}=(1-Y)\left(\frac{\mathrm{d}\phi}{\mathrm{d}Z}\right)_{S1}+Y\left(\frac{\mathrm{d}\phi}{\mathrm{d}Z}\right)_{S2}\,,$$

$$\left(\frac{\mathrm{d}\phi}{\mathrm{d}Z}\right)_{S1}=-\left(\frac{1}{3-Y}+\frac{1}{2-Y}+\frac{1}{1+Y}\right)\frac{1}{\Delta Z}\phi_{m}$$
$$+\frac{(2-Y)(3-Y)}{2(1-Y)}\frac{1}{\Delta Z}\phi_{mp+1}$$

$$-\frac{(1-Y)(3-Y)}{2-Y}\frac{1}{\Delta Z}\phi_{mp+2}$$

$$+\frac{(1-Y)(2-Y)}{2(3-Y)}\frac{1}{\Delta Z}\phi_{mp+3},$$

$$\left(\frac{d\phi}{dZ}\right)_{S2}=-\left(\frac{1}{3-Y}+\frac{1}{3-Y}+\frac{1}{2-Y}\right)\frac{1}{\Delta Z}\phi_m$$

$$+\frac{(3-Y)(4-Y)}{2(2-Y)}\frac{1}{\Delta Z}\phi_{mp+2}$$

$$-\frac{(2-Y)(4-Y)}{3-Y}\frac{1}{\Delta Z}\phi_{mp+3}$$

$$+\frac{(2-Y)(3-Y)}{2(4-Y)}\frac{1}{\Delta Z}\phi_{mp+4}.$$

Acknowledgement

This research was supported by a subcontract from Grumman Aerospace Corporation on Contract NaS8-32948 from the National Aeronautics and Space Administration. We wish to thank Dr. David Larson of Grumman for helpful discussions and encouragement.

Nomenclature

- a Radius of the ampoule [m]
- b Thickness of the insulation [m]
- C_p Heat capacity [J/kg · K]
- h Heat transfer coefficient [W/m² · K]
- h_c Heat transfer coefficient in the cooler [W/m² · K]
- h_h Heat transfer coefficient in the heater [W/m² · K]
- H^{cL} Biot number in the cooler, $h_c a/k^L$
- H^{hL} Biot number in the heater, $h_h a/k^L$
- H^{Lm} Geometric mean of H^{hL} and H^{cL}
- ΔH Latent heat of solidification [J/kg]
- i Integer denoting grid point in space coordinate
- I Dimensionless thickness of insulation, b/a
- j Integer denoting grid point in time coordinate
- k Thermal conductivity [W/m · s]
- k^L Thermal conductivity in liquid at melting temperature [W/m · K]
- k^S Thermal conductivity in solid at melting temperature [W/m · K]
- K Ratio of thermal conductivity in solid to that in liquid
- P Interfacial position parameter $(\bar{\delta}_2 - \bar{\delta})/(\bar{\delta}_2 - \bar{\delta}_1)$
- Pe^L Peclet number, $vC_p\rho a/k^L$
- Pe^{L1} Peclet number before the change of ampoule moving rate, $V_1C_p\rho a/k^L$
- Pe^{L2} Peclet number after the change of ampoule moving rate, $V_2C_p\rho a/k^L$
- t Time [s]
- T Temperature [K]
- T_a Temperature of environment [K]
- T_c Temperature of the cooler [K]
- T_h Temperature of the heater [K]
- T_m Temperature of the solid/liquid interface [K]
- V Ampoule moving rate [m/s]
- V_1 Ampoule moving rate before the change [m/s]
- V_2 Ampoule moving rate after the change [m/s]
- V_s Solidification rate [m/s]
- W_h Dimensionless latent heat, $\Delta H/C_p(T_h - T_c)$
- Y Ratio of ϵ to Δz
- z Space coordinate [m]
- Δz Grid spacing in space coordinate [m]
- Z Dimensionless space coordinate, z/a
- ΔZ Dimensionless grid spacing in space coordinate
- δ Interface position relative to the center of the insulation [m]
- $\bar{\delta}$ Dimensionless interface position, δ/a
- $\bar{\delta}_1$ Dimensionless interface position before the change of ampoule moving rate
- $\bar{\delta}_2$ Dimensionless interface position after the change of ampoule moving rate
- $\Delta\bar{\delta}$ Dimensionless interface movement in each time step $\Delta\theta$
- ϵ Distance between the mp^{th} grid point and the solid/liquid interface
- ρ Density [kg/m³]
- θ Dimensionless time, $k^L t/C_p\rho a^2$
- $\Delta\theta$ Dimensionless time step
- ϕ Dimensionless temperature, $(T - T_c)/(T_h - T_c)$
- ϕ^a Dimensionless temperature of environment, $(T_a - T_c)/(T_h - T_c)$
- ϕ_m Dimensionless interface temperature, $(T_m - T_c)/(T_h - T_c)$

References

[1] K.A. Jackson and J.D. Hunt, Trans. AIME 236 (1966) 1129.
[2] B. Toloui and A. Hellawell, Acta Met. 24 (1976) 565.
[3] D.J. Larson, Jr., private communication.
[4] M.M. Farag, R. Matera and M.C. Flemings, Met. Trans. 10B (1979) 381.
[5] P.S. Ravishankar and T.-W. Fu, to be published.
[6] Ta-Wei Fu, Ph.D. thesis, Clarkson College of Technology (1981).
[7] SAS User's Guide (SAS) Institute Inc., Raleigh, North Carolina, 1979) p. 237.
[8] T.-W. Fu and W.R. Wilcox, J. Crystal Growth 48 (1980) 416.